

CONVERGENCE AND GAUGE DEPENDENCE
PROPERTIES OF THE RESUMMED ONE-LOOP
QUARK–QUARK SCATTERING AMPLITUDE
IN PERTURBATIVE QCD

J. H. Field

Département de Physique Nucléaire et Corpusculaire, Université de Genève, Switzerland

| | |
|--|-----|
| INTRODUCTION | 676 |
| THE QUARK–QUARK SCATTERING AMPLITUDE TO $O(\alpha_s^2)$ IN AN ARBITRARY COVARIANT GAUGE | 677 |
| THE RESUMMED QUARK–QUARK SCATTERING AMPLITUDE | 681 |
| SELF-SIMILARITY PROPERTIES OF α_s^{eff} AND THE RENORMALIZATION GROUP | 685 |
| DISCUSSION | 688 |
| REFERENCES | 701 |

CONVERGENCE AND GAUGE DEPENDENCE PROPERTIES OF THE RESUMMED ONE-LOOP QUARK–QUARK SCATTERING AMPLITUDE IN PERTURBATIVE QCD

J. H. Field

Département de Physique Nucléaire et Corpusculaire, Université de Genève, Switzerland

The one-loop QCD effective charge α_s^{eff} for quark–quark scattering is derived by diagrammatic resummation of the one-loop amplitude using an arbitrary covariant gauge. Except for the particular choice of gauge parameter $\xi = -3$, α_s^{eff} is found to *increase* with increasing physical scale, Q , as $\ln Q$ or $\ln^2 Q$. For $\xi = -3$, α_s^{eff} decreases with increasing Q and satisfies a renormalization group equation. Also, except for the case $\xi = 19/9$, convergence radii of geometric series are found to impose upper limits on Q .

Однопетлевой эффективный заряд КХД α_s^{eff} кварк–кваркового рассеяния найден с помощью суммирования однопетлевой амплитуды с использованием произвольной калибровки. За исключением специального выбора калибровочного параметра $\xi = -3$ найдено, что α_s^{eff} растет с увеличением физического масштаба Q пропорционально $\ln Q$ или $\ln^2 Q$. Для случая $\xi = -3$ α_s^{eff} уменьшается с увеличением Q и удовлетворяет уравнению ренормализационной группы. Помимо этого найдено, что за исключением случая $\xi = 19/9$ радиусы сходимости геометрического ряда налагают верхние пределы на Q .

PACS: 12.38-t, 12.38.Bx, 12.38.Cy

INTRODUCTION

Quark–quark scattering in the next-to-leading order QCD has been calculated by several different groups [1–4]. Coqueraux and De Rafael [1] calculated the one-loop corrections to the invariant amplitude in the Feynman gauge using an on-shell renormalization scheme [5]. In [2–4] complete expressions for the squared invariant amplitude were given in the dimensional regularization scheme [6]. The calculations presented in the present paper generalize those of [1–4] in two ways:

- (i) An arbitrary covariant gauge is considered.
- (ii) The one-loop ultra-violet (UV) divergent loop and vertex diagrams are resummed to all orders in α_s .

The procedure of (ii) yields a scale-dependent «effective charge» as a factor in the invariant amplitude. The resummation is done, not by solving a renormalization group equation (RGE), but by an exact sum of the relevant diagrams to give the QCD analogue of the Dyson sum of QED.

The results are very surprising. The effective charge is gauge-dependent at $O(\alpha_s^3)$ and beyond, and except for one specific choice of gauge, does not display «asymptotic freedom» but instead *increases* as $\ln Q$ or $\ln^2 Q$ at large scales Q . Only for the same special choice of gauge, where contributions from vertex diagrams vanish, does the effective charge satisfy a RGE of the type that is valid in QED [7–11]. For this special choice of gauge (called «loop gauge») the effective charge decreases with increasing scale, but only to a fixed limit Q_L , determined by the convergence radius of the geometric sum of gluon and fermion loops in the dressed gluon propagator. The measured value of α_s suggests that $Q_L \simeq 300$ GeV, already of phenomenological importance at the Fermilab $p\bar{p}$ collider.

The plan of the paper is as follows. In the next Section the UV divergent (before renormalization) one-loop corrections to the quark–quark scattering amplitude in Feynman gauge are derived from similar corrections to the quark–quark–gluon vertex given in [12]. The generalization to an arbitrary covariant gauge is made using results reported in [13]. In Sec. 2 the one-loop corrections are diagrammatically resummed to yield the QCD analogue of the Dyson sum of QED. In Sec. 3 the self-similarity and renormalization group properties of the effective charge derived in Sec. 2 are discussed. In the final Section the classical proofs of the asymptotic freedom property of QCD in the literature are critically examined in the light of the results obtained in the previous Sections. Also, briefly discussed are: (i) «renormalons», (ii) the generalization to higher loop order vacuum polarization and vertex corrections, and (iii) pinch technique and related calculations of proper self-energy and vertex functions, both in QCD and in the Standard Electroweak Model (SEM).

The present paper is the fifth in a series on fundamental physics aspects of perturbative QED and QCD: [15] discusses on-shell renormalization and optimized perturbation theory in QED and QCD; [16] considers the role of non-vanishing fermion or gluon masses as physical regulators for diagrams with combined infrared (IR) and ultra-violet (UV) divergences; the relation of such IR/UV divergent diagrams to the Lee–Nauenberg [17] and Kinoshita [18] theorems of QED and QCD is examined in [19]; convergence conditions for resummed physical amplitudes, as discussed in the present paper for quark–quark scattering in QCD, are analyzed for the analogous QED case of scattering of unequal mass charged fermions in [20].

1. THE QUARK–QUARK SCATTERING AMPLITUDE TO $O(\alpha_s^2)$ IN AN ARBITRARY COVARIANT GAUGE

The process considered is the scattering of two equal mass quarks through an angle of 90° in their CM system. The lowest order diagram is shown in Fig. 1, *a*. The four-vectors of the incoming (outgoing) quarks are p_1, p_2 (p_3, p_4). In this

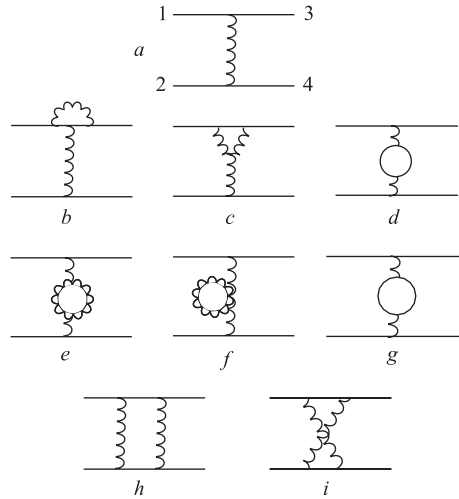


Fig. 1. Diagrams contributing to $\mathcal{M}^{(\text{LO})}$. Solid lines denote quarks, wavy lines — gluons and the closed loop in g — ghosts

configuration the exchanged gluon has a virtuality $t = -s/2$ where

$$t \equiv (p_1 - p_3)^2 = u \equiv (p_1 - p_4)^2, \quad (1.1)$$

$$s \equiv (p_1 + p_2)^2 = (p_3 + p_4)^2. \quad (1.2)$$

Denoting the invariant amplitude corresponding to the diagram in Fig. 1, a by $\mathcal{M}^{(0)}$ (quark spin and color indices are suppressed), the $O(\alpha_s^2)$ amplitude may be written as

$$\mathcal{M}^{(1)} = \mathcal{M}^{(0)} \sum_i \mathcal{A}_i, \quad (1.3)$$

where the one-loop virtual corrections \mathcal{A}_i are given by the diagrams shown in Fig. 1, $b-i$. Three topologically distinct types of diagrams occur:

- vertex corrections as in Fig. 1, b, c and the two similar diagrams given by the exchange $13 \leftrightarrow 24$;
- loop corrections (Fig. 1, $d-g$);
- box diagrams (Fig. 1, h, i).

The leading logarithmic corrections, \mathcal{A}_i , corresponding to the contributions of diagrams that are UV divergent before renormalization, have been derived in a straightforward fashion from the corrections to the quark–quark–gluon vertex presented in [12]. The results, in Feynman gauge, derived using dimensional

Table 1. UV divergent (before renormalization) one-loop virtual corrections, at leading logarithmic accuracy, to the 90° quark–quark scattering amplitude in Feynman gauge

| i | Diagram in Fig. 1 | Type | $(\alpha_s^\mu/\pi)^{-1} \times$ correction factor, A_i , to $\mathcal{M}^{(0)}$ |
|-----|------------------------------|-----------------------|--|
| 1 | $b) + 13 \leftrightarrow 24$ | Abelian vertex | $\frac{C_A}{2} \ln \frac{Q}{\mu}$ |
| 2 | $c) + 13 \leftrightarrow 24$ | Non-Abelian vertex | $-\frac{3C_A}{2} \ln \frac{Q}{\mu}$ |
| 3 | $d)$ | Quark loops | $\frac{n_f}{3} \ln \frac{Q}{\mu}$ |
| 4 | $e) + f) + g)$ | Gluon and ghost loops | $-\frac{5C_A}{6} \ln \frac{Q}{\mu}$ |

regularization [6] are presented in Table 1*. Here $Q = \sqrt{-t} = \sqrt{s/2}$ is the physical scale, and μ is the renormalization subtraction scale. C_A is the usual QCD color factor ($C_A = \text{number of colors} = 3$), while n_f is the number of light quark flavors contributing to the vacuum polarization loops in Fig. 1, d . α_s^μ is the square of the renormalized on-shell strong coupling constant at the scale μ . The corrections \mathcal{A}_1 – \mathcal{A}_4 may be combined to yield a term proportional to the first coefficient in the perturbation series in α_s of the beta function of QCD. Denoting the quark loop + gluon loop + ghost loop correction, $\mathcal{A}_3 + \mathcal{A}_4$, by \mathcal{L}^μ , and the vertex correction, $\mathcal{A}_1 + \mathcal{A}_2$, by \mathcal{V}^μ , and generalizing to an arbitrary covariant gauge specified by the parameter ξ , in which the gluon propagator is written as

$$P^{\mu\nu}(q^2) = -\frac{i}{q^2} \left[g^{\mu\nu} - (1 - \xi) \frac{q^\mu q^\nu}{q^2} \right], \quad (1.4)$$

*In two previous versions of the present paper [21] the one-loop corrections to the quark–quark scattering amplitude were taken from Table 1 of [1]. This calculation was performed using on-shell normalization [5] in which explicit quark and gluon mass parameters were introduced. Comparison of the results of [1] with those of [12] and [13] and those for the related QED Bhabha scattering process [22] has revealed a number of inconsistencies with the results of [1]. (i) The «Vertex($a + b$)» contribution shown is simply the QED result modified by a single multiplicative color factor. The QCD-specific UV divergent term found in [12] and [13] and presented in the first row of Table 1 in the present paper is absent. (ii) The «Three Gluon($i + j$)» contribution should, according to [12], be $3y/2$, not $-y$. (iii) Adding up the singly logarithmic terms of Table 1 of [1] yields, as the coefficient of the logarithm of the physical scale, β_0 , but the contribution of «Vertex(a and b)» actually corresponds, not to a UV divergent term, but to an IR divergent one, that is canceled on adding the contributions of diagrams with real gluon radiation from the external quark lines. Thus, Eqs. (2.4) and (2.5) of the previous versions of the present paper were incorrect and the appearance of β_0 in Eq. (2.12) was fortuitous. However, Eqs. (1.5) and (1.6) of the present revised and corrected version are identical to Eqs. (2.15) and (2.16) of the previous versions, so that none of the subsequent discussion or conclusions are affected by the corrections.

yields the explicit gauge dependence* of \mathcal{V}^μ and \mathcal{L}^μ [13]

$$\mathcal{V}^\mu(\xi) = -\frac{\alpha_s^\mu}{\pi} \frac{3}{4} (3 + \xi) \ln\left(\frac{Q}{\mu}\right), \quad (1.5)$$

$$\mathcal{L}^\mu(\xi) = \frac{\alpha_s^\mu}{\pi} \left[-\frac{3}{4} \left(\frac{13}{3} - \xi \right) + \frac{n_f}{3} \right] \ln\left(\frac{Q}{\mu}\right). \quad (1.6)$$

Adding Eqs. (1.5) and (1.6):

$$\mathcal{V}^\mu(\xi) + \mathcal{L}^\mu(\xi) = -\frac{\alpha_s^\mu}{\pi} \left(\frac{11}{2} - \frac{n_f}{3} \right) \ln\left(\frac{Q}{\mu}\right) = -\frac{\alpha_s^\mu}{\pi} \beta_0 \ln\left(\frac{Q}{\mu}\right), \quad (1.7)$$

where β_0 is the first coefficient of the QCD β function [$a_s \equiv \alpha_s/\pi$]:

$$\mu \frac{\partial a_s}{\partial \mu} = \beta(a_s) = -\beta_0 a_s^2 + \dots \quad (1.8)$$

To $O(\alpha_s^2)$, α_s^Q may be identified with the solution, $\alpha_s^{\text{RGE}}(Q)$, of the RGE (1.8):

$$\begin{aligned} \mathcal{M}^{\text{LO}} &= \mathcal{M}^{(0)} + \mathcal{M}^{(1)} = \mathcal{M}^{(0)} (1 + \mathcal{V}^\mu(\xi) + \mathcal{L}^\mu(\xi)) = \\ &= \frac{\mathcal{M}^{(0)}}{\alpha_s^\mu} \left[\alpha_s^\mu \left[1 - \frac{\alpha_s^\mu}{\pi} \beta_0 \ln\left(\frac{Q}{\mu}\right) \right] \right] = \frac{\mathcal{M}^{(0)} \alpha_s^{\text{RGE}}(Q)}{\alpha_s^\mu} + O((\alpha_s^\mu)^2), \end{aligned} \quad (1.9)$$

where

$$\alpha_s^{\text{RGE}}(Q) = \alpha_s^Q = \frac{\alpha_s^\mu}{1 + \frac{\alpha_s^\mu}{\pi} \beta_0 \ln\left(\frac{Q}{\mu}\right)}, \quad (1.10)$$

\mathcal{M}^{LO} denotes the amplitude including Leading Order (LO) vertex and vacuum polarization corrections. In the following section the amplitude $\mathcal{M}^{(\infty)}$, in which these corrections are summed to all orders in α_s , is derived.

It can be seen that, at one loop, the gauge invariant result (1.7) is obtained on adding the UV divergent contributions of diagrams b – g in Fig. 1. The box diagrams h and i and those obtained by exchanging the internal quark and gluon propagators, form, together with the diagrams where a single gluon is radiated from one of the external quark lines of Fig. 1, a , another gauge invariant set. Indeed the contribution to the cross section of this set of diagrams, which involve only Abelian quark–gluon couplings, is obtained by multiplying the result for the analogous QED t -channel Bhabha scattering process [22] by the appropriate

*This gauge dependence of one-loop vertex and vacuum polarization insertions containing triple gauge boson couplings is universal for all non-Abelian gauge theories. See, for example, [14, Eqs. (12.114) and (12.122)].

QCD color factor: $C_2(N_c) = (N_c^2 - 1)/2N_c = 4/3$. The contribution of the box diagrams alone is UV finite, but IR divergent for the case of massless gluons. This IR divergence is canceled on adding the contribution of the real gluon radiation diagrams. The contributions of the box diagrams and the real radiation diagrams are however, separately, gauge invariant*. Since the box diagrams are UV finite, and so do not require renormalization, they do not contribute to the QCD effective charge. All the terms that contribute to the latter at one loop are presented in Table 1; they are UV divergent before renormalization.

2. THE RESUMMED QUARK–QUARK SCATTERING AMPLITUDE

The topographical structures** of the diagrams that modify the gluon propagator in the quark–quark scattering amplitude at $O(\alpha_s^2)$, $O(\alpha_s^3)$ and $O(\alpha_s^4)$ are shown in Fig. 2, *a, b, c*, respectively. V and L denote vertex and loop (vacuum polarization) contributions:

$$V = V_1 + V_2, \quad (2.1)$$

$$L = \sum_{i=1}^{n_f} F_i + G_1 + G_2 + G_3. \quad (2.2)$$

V_1, V_2 correspond to the diagrams in Fig. 1, *b, c*; $\sum_{i=1}^{n_f} F_i$ to Fig. 1, *d* and G_1, G_2, G_3 to Fig. 1, *e, f, g*. In the case that only one vertex insertion occurs there is a factor 2 for the two ends of the gluon propagator. Since the propagator has only two ends the vertex corrections are never higher than quadratic in the perturbation series for the amplitude. Although the topographical structure of diagrams containing vertex corrections is different at $O(\alpha_s^3)$ than at $O(\alpha_s^2)$ it remains the same at all higher orders. The all-orders resummed amplitude is

$$\begin{aligned} \mathcal{M}^{(\infty)} &= \mathcal{M}^{(0)} [1 + 2V + L + V^2 + 2VL + L^2 + V^2L + 2VL^2 + L^3 + \dots] = \\ &= \mathcal{M}^{(0)} [1 + L + L^2 + \dots + V^2 (1 + L + L^2 + \dots + 2V(1 + L + L^2 + \dots))] = \\ &= \frac{\mathcal{M}^{(0)}(1 + V)^2}{1 - L}. \end{aligned} \quad (2.3)$$

*See [23] for a complete diagrammatic discussion of gauge cancellations in the one-loop corrected quark–quark scattering amplitude.

**The use of the word «topographical structure» to indicate a particular disposition of vertex and (possibly resummed) self-energy insertions in a diagram is deliberate. Diagrams with internal lines in the vertex or self-energy insertions have a different topology but the same topography as the one-loop diagrams shown in Fig. 2.

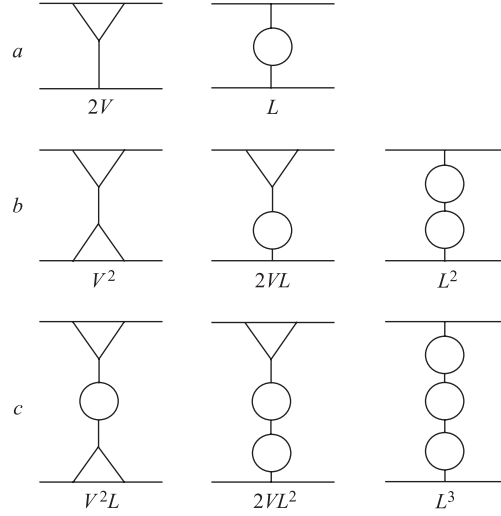


Fig. 2. The topographical structure of diagrams contributing to the resummed quark–quark scattering amplitude: *a*) $O(\alpha_s^2)$; *b*) $O(\alpha_s^3)$; *c*) $O(\alpha_s^4)$. In diagrams containing only one vertex insertion the contribution given by the exchange $13 \leftrightarrow 24$ (see Fig. 1) is understood to be included

In an arbitrary covariant gauge with momentum subtraction at scale μ , and in leading logarithmic approximation, $V = \mathcal{V}^\mu(\xi)/2$, $L = \mathcal{L}^\mu(\xi)$ so that

$$\mathcal{M}^{(\infty)} = \frac{\mathcal{M}^{(0)} \alpha_s^{\text{eff}}(Q)}{\alpha_s^\mu} = \frac{\mathcal{M}^{(0)} \left(1 + \frac{1}{2} \mathcal{V}^\mu(\xi)\right)^2}{1 - \mathcal{L}^\mu(\xi)} \quad (2.4)$$

leading to the following expression, in leading logarithmic approximation, for the resummed one-loop effective charge:

$$\alpha_s^{\text{eff}}(Q) = \alpha_s^\mu \frac{\left[1 - \frac{3\alpha_s^\mu}{8\pi} (3 + \xi) \ln\left(\frac{Q}{\mu}\right)\right]^2}{1 + \frac{\alpha_s^\mu}{4\pi} \left[13 - 3\xi - \frac{4n_f}{3}\right] \ln\left(\frac{Q}{\mu}\right)}. \quad (2.5)$$

The conventional one-loop QCD running coupling constant Eq. (1.10) is recovered only for the special choice of gauge parameter $\xi = \xi_L = -3$ («loop gauge»). Only in this case does $\alpha_s^{\text{eff}}(Q)$ decrease monotonically with increasing Q . For any other choice of gauge $\alpha_s^{\text{eff}}(Q)$ does not show «asymptotic freedom» as $Q \rightarrow \infty$ but instead *increases* as $\ln Q$ when $\xi \neq \xi_V$ and as $\ln^2 Q$ when $\xi = \xi_V$. The

choice $\xi = \xi_V$ («vertex gauge») where

$$\xi_V = (39 - 4n_f)/9$$

corresponds to a vanishing coefficient of $\ln(Q/\mu)$ in the denominator of Eq. (2.5). As discussed in more detail below, only in loop gauge is the equation for the effective charge «self-similar» like the effective charge in QED or the solution (1.10) of the RGE Eq. (1.8). Even in loop gauge the effective charge of Eq. (2.5) does not decrease without limit as $Q \rightarrow \infty$. The maximum possible scale Q_L (Landau scale) is determined by the convergence properties of the geometric sum that yields the denominator of Eq. (2.5). The geometric series is convergent provided that $|L| < 1$ [24]. This implies that

$$\left| \frac{\alpha_s^\mu}{4\pi} \left[13 - 3\xi - \frac{4n_f}{3} \right] \ln \left(\frac{Q}{\mu} \right) \right| < 1. \quad (2.6)$$

The corresponding Landau scale is then

$$Q_L = \mu \exp \left[\frac{4\pi}{\alpha_s^\mu \left[13 - 3\xi - \frac{4n_f}{3} \right]} \right] \quad (2.7)$$

and

$$\alpha_s^{\text{eff}}(Q_L) = \frac{\alpha_s^\mu}{2} \left[1 - \frac{3\alpha_s^\mu}{8\pi} (3 + \xi) \ln \left(\frac{Q_L}{\mu} \right) \right]^2. \quad (2.8)$$

For $\xi = -3$:

$$\alpha_s^{\text{eff}}(Q_L) = \frac{\alpha_s^\mu}{2}, \quad (2.9)$$

so the convergence condition (2.6) implies that in this case α_s^{eff} cannot evolve down by more than a factor of 1/2 of its initial value before Eq. (2.5) diverges — there is no «asymptotic freedom». The convergence conditions for a geometric series with a negative common ratio, such as that which generates the QCD running coupling constant, are derived below in Appendix. Unlike in the case of the Landau pole [25] of QED, with a positive common ratio, $r = |r|$, where the running coupling constant is proportional to $1/(1 - |r|)$, it is not obvious, by inspection, that the QCD perturbation series is *not* equal to $1/(1 + |r|)$ when $|r| > 1$. However, (see Appendix) this is quite clear from the exact formula, Eq. (A.1), giving the sum for any finite number of terms. Physicists have the right to be as free as possible in making conjectures in their attempts to describe nature in the simplest way possible, but not to make ones that are contrary to mathematical laws.

Table 2. Values of the Landau scale Q_L (convergence limit) of the QCD effective charge for $\mu = 5$ GeV, $\alpha_s^\mu = 0.2$, $n_f = 5$

| Gauge | Feynman ($\xi = 1$) | Landau ($\xi = 0$) | Loop ($\xi = -3$) | Vertex ($\xi = 19/9$) |
|-------------|-----------------------|----------------------|---------------------|-------------------------|
| Q_L , GeV | $7.68 \cdot 10^8$ | $1.02 \cdot 10^5$ | 301 | ∞ |

Numerical values of Q_L for $\mu = 5$ GeV, $\alpha_s^\mu = 0.2$ and $n_f = 5$ (corresponding, approximately, to the experimental value of α_s^μ) and four different choices of gauge parameter are presented in Table 2. For loop gauge ($\xi = -3$) Q_L is only 300 GeV, with phenomenological consequences perhaps already at the Fermilab $p\bar{p}$ collider, but certainly at the future LHC pp collider. It may be noted that, in all cases except vertex gauge, Q_L lies well below the Grand Unification (GUT) scale of $\simeq 10^{15}$ GeV. Since for any gauge choice except $\xi = -3$, α_s^{eff} diverges as $\ln Q$ or $\ln^2 Q$ at large Q , there can be no «unification» [26, 27] of the strong and electromagnetic interactions at large scales Q , for any choice of gauge parameter, at least if the running strong coupling constant is identified with an effective charge such as that in Eq. (2.5). In fact, all studies, to date, of Grand Unification have implicitly used loop gauge where the maximum scale Q_L is only $\simeq 300$ GeV. In vertex gauge, since all vacuum polarization contributions vanish, there is no convergence limitation on Q in Eq. (2.5).

The behavior of α_s^{eff} at large values of Q depends on the value of the Landau scale and value, Q_0 , of Q at which the numerator of Eq. (2.5) vanishes:

$$Q_0 = \mu \exp \left[\frac{8\pi}{3\alpha_s^\mu(3 + \xi)} \right]. \quad (2.10)$$

The value of ξ , ξ_0 , at which Q_L and Q_0 are equal, is given by (2.7) and (2.10) as

$$\xi_0(n_f) = \frac{1}{9} \left(17 - \frac{8n_f}{3} \right). \quad (2.11)$$

For $n_f = 5$, $\xi_0 = 0.4074\dots$ When $\xi < \xi_0$ (e.g., Loop and Landau gauges) and $Q_L < Q_0$, then α_s^{eff} diverges before vanishing and so decreases monotonically with increasing Q within its convergence radius. For $\xi > \xi_0$ (e.g., Feynman and Vertex gauges), $Q_L > Q_0$. In this case α_s^{eff} first decreases with increasing Q , reaching a minimum value at zero, and then increases with increasing Q up to Q_L . In vertex gauge Q_L is infinite. Numerical values of Q_0 for the same parameter choices as in Table 2 are presented in Table 3. The scale Q_0 is defined (i.e., $Q_L > Q_0$) only for Feynman gauge ($Q_0 = 176$ TeV) and Vertex gauge ($Q_0 = 18.1$ TeV).

The diagrams shown in Fig. 2 each contain only a single «dressed» virtual gluon. It is also possible to consider cases in which the substitution of the series of diagrams illustrated in Fig. 2, and summed in Eq. (2.3), is made in a diagram

Table 3. Values of Q_0 (the scale at which $\alpha_s^{\text{eff}}(Q)$ vanishes). Parameters as in Table 2

| Gauge | Feynman ($\xi = 1$) | Landau ($\xi = 0$) | Loop ($\xi = -3$) | Vertex ($\xi = 19/9$) |
|-------------|-----------------------|----------------------|---------------------|-------------------------|
| Q_0 , TeV | 176 | Undefined | Undefined | 18.1 |

containing more than one virtual gluon (for example, the box diagrams shown in Fig. 1, h and i). This will result in a further higher order correction to the quark–quark scattering process. It is clear, however, that the manifest gauge dependence of the resummed one-loop contribution will be unaffected by the presence of other virtual gluons («dressed» or not) in the diagram. Every virtual gluon has only two ends, and so the resummed vertex correction is at most quadratic. Then no cancellation is possible of the gauge-dependent pieces of multiple vacuum polarization insertions. However, as further discussed in Sec. 4 below, the box diagrams themselves can be resummed. This typically results in a Sudakov-like double logarithm, not a geometric series as found for resummed vacuum polarization diagrams.

3. SELF-SIMILARITY PROPERTIES OF α_s^{eff} AND THE RENORMALIZATION GROUP

Introducing the abbreviated notation:

$$v(\xi) \equiv \frac{3}{8}(3 + \xi), \quad l(\xi) = \frac{1}{4} \left[13 - 3\xi - \frac{4n_f}{3} \right],$$

$$\alpha_s^{\text{eff}}(Q)/\pi \equiv a_Q, \quad \alpha_s^\mu/\pi \equiv a_\mu, \quad \lambda \equiv \ln(Q/\mu),$$

Eq. (2.5) may be written as

$$a_Q = \frac{a_\mu [1 - a_\mu v(\xi)\lambda]^2}{1 + a_\mu l(\xi)\lambda}. \quad (3.1)$$

With $\xi = -3$, $v(-3) = 0$, Eq. (3.1) becomes

$$a_Q = \frac{a_\mu}{1 + a_\mu l(-3)\lambda}. \quad (3.2)$$

Equation (3.2) is the solution of a one-loop RGE similar to that for the QED effective charge [10, 11]:

$$\frac{Q}{a_Q} \frac{\partial a_Q}{\partial Q} = -l(-3)a_Q = -\beta_0 a_Q, \quad (3.3)$$

where

$$\beta_0 = l(-3) = \frac{11}{2} - \frac{n_f}{3}. \quad (3.4)$$

For a gauge choice such that $v \neq 0$, the partial differential equation satisfied by a_Q is

$$\frac{Q}{a_Q} \frac{\partial a_Q}{\partial Q} = -a_Q \left[\frac{l(\xi)}{(1 - a_\mu v(\xi)\lambda)^2} + 2 \frac{v(\xi)(1 + a_\mu l(\xi)\lambda)}{(1 - a_\mu v(\xi)\lambda)^3} \right], \quad (3.5)$$

so that, in this case, the effective charge a_Q does not satisfy the RGE (3.3). Expanding in powers of a_μ on the right-hand side of Eq. (3.5) gives

$$\frac{Q}{a_Q} \frac{\partial a_Q}{\partial Q} = -a_Q [l(\xi) + 2v(\xi) + O(a_\mu)], \quad (3.6)$$

$$= -a_Q [\beta_0 + O(a_\mu)]. \quad (3.7)$$

Thus, neglecting terms of $O(a_Q a_\mu) \simeq O(a_\mu^2)$, so that only the first term in the QCD perturbation series is retained, $a_Q \rightarrow a_Q^{(1)}$ and it can be seen that $a_Q^{(1)}$, for an arbitrary gauge choice, satisfies the same partial differential equation as the one-loop all orders resummed a_Q in loop gauge. The relation of this result to the previous derivations of the QCD running coupling constant, where it has generally been conjectured that a gauge invariant result is obtained to all orders in perturbation theory, is discussed in the following Section.

Equation (3.2) is self-similar in the sense that for any values of μ and Q the equation defined by the exchange $\mu \leftrightarrow Q$ is identical to the original equation. A consequence of this symmetry property is that a_Q in Eq. (3.2) is independent of μ (with the important caveat that, since the denominator is the sum to infinity of a geometric series, μ must be such that $|a_\mu l(-3)\lambda| < 1$), and that in the equation with $\mu \leftrightarrow Q$, a_μ is independent of Q . This is the mathematical basis of the Renormalization Group [7–9]. Such a universal self-similarity property is not, however, shared by Eq. (3.1) when $v(\xi) \neq 0$.

Equation (3.1) is self-similar under the exchange $\mu \leftrightarrow Q$ provided that the equation

$$a_\mu = \frac{a_Q [1 + a_Q v(\xi)\lambda]^2}{1 - a_Q l(\xi)\lambda} \quad (3.8)$$

and Eq. (3.1) are both valid. Simultaneous solution of Eqs. (3.1), (3.8) in the case that $v(\xi) \neq 0$ leads to a quadratic equation for a_μ with the solution:

$$a_\mu = \frac{1}{v(\xi)\lambda} + \frac{a_Q}{2} \pm \frac{1}{2} \sqrt{\left(\frac{2}{v(\xi)\lambda} + a_Q \right) \left(\frac{2}{v(\xi)\lambda} - 3a_Q \right)}. \quad (3.9)$$

Real solutions of Eq. (3.9) exist provided that either

$$\frac{2}{3v(\xi)\lambda} > a_Q > -\frac{2}{v(\xi)\lambda} \quad (3.10)$$

(both factors under the square root positive) or

$$\frac{3v(\xi)\lambda}{2} > \frac{1}{a_Q} > -\frac{v(\xi)\lambda}{2} \quad (3.11)$$

(both factors under the square root negative).

The solution for a_μ , Eq. (3.9), is independent of $l(\xi)$. Thus, for fixed values of a_Q , Q , μ , $v(\xi) \neq 0$, satisfying the conditions (3.10) or (3.11), there are, in general, two values of a_μ such that Eq. (3.1) is self-similar. This value of a_μ has, however, no relation to the effective charge at the scale μ given by Eq. (3.1) when $Q = \mu$. Choosing $Q = 90$ GeV and Landau gauge, then (see Fig. 3) $a_Q = 0.095/\pi = 0.0302$. The choice $\mu = 5$ GeV gives $2/(v(0)\lambda) = 1.933$. The a_Q terms under the square root of Eq. (3.9) may then be neglected, leading to the solutions

$$a_\mu^+ \simeq \frac{2}{v(0)\lambda} + \frac{a_Q}{2} = 1.9648, \quad a_\mu^- \simeq \frac{a_Q}{2} = 0.0152$$

to be compared with the physical value:

$$a_\mu = \alpha^{\text{eff}}(5 \text{ GeV})/\pi = 0.2/\pi = 0.064.$$

Unlike for the special case $v = 0$, the first derivative of a_Q in general depends on the scale μ . For $Q = \mu$ the derivative is a negative constant fixed by the first coefficient in the perturbation series for the beta function as in Eq. (3.3). For

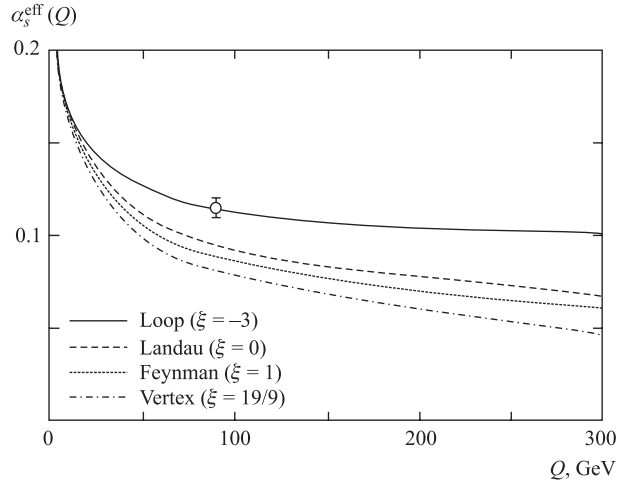


Fig. 3. The variation of the Effective Charge (2.5) with the scale Q for different choices of the gauge parameter ξ . $5 < Q < 300$ GeV ($\alpha_s^{\text{eff}}(5 \text{ GeV}) = 0.2$, $n_f = 5$). The error bars (± 0.005) on the point at $Q = 90$ GeV on the loop gauge curve are typical of those on an α_s measurement using hadronic Z decays [65]

any other choice of μ when $v \neq 0$ the derivative varies with Q and μ according to Eq. (3.5). Thus, if the effective charge is parametrized in terms of a_μ , $a_{\mu'}$ at the reference scale Q_R :

$$a_{Q_R} = a_\mu \frac{[1 - a_\mu v(\xi)\lambda_R]}{[1 + a_\mu l(\xi)\lambda_R]} = a_{\mu'} \frac{[1 - a_{\mu'} v(\xi)\lambda'_R]}{[1 + a_{\mu'} l(\xi)\lambda'_R]}, \quad (3.12)$$

$$\lambda_R \equiv \ln(Q_R/\mu), \quad \lambda'_R \equiv \ln(Q_R/\mu'),$$

then for $Q \neq Q_R$ and $v(\xi) \neq 0$ the effective charge a_Q predicted by the formula containing μ (the second member of Eq. (3.12)) will be different to that predicted by that containing μ' (the third member of Eq. (3.12)), so that the value of a_Q depends upon the choice of renormalization scale — it is no longer invariant. Renormalization group invariance with respect to the choice of the scale μ is therefore not respected unless $v(\xi) = 0$, i.e., $\xi = -3$.

4. DISCUSSION

In the original derivations of the «asymptotic freedom» property of QCD [28, 29] no calculations were performed beyond the lowest nontrivial order, $O(\alpha_s^2)$, and no actual amplitudes for physical processes were considered. It was conjectured (without any check by direct diagrammatic calculation) that the QCD running coupling constant (RCC) could, in general (for any choice of gauge), be identified with the solution of the differential equation (1.8). The one-loop QCD beta function was calculated by considering the Callan–Symanzik [10, 11] equation for an irreducible n -point function (typically the gluon–quark–quark vertex or the triple gluon vertex). Calculation of the anomalous dimensions of the quark and gluon fields then yields the (gauge invariant) expression for the first beta function coefficient β_0 in Eq. (1.8) above. An analogous result is obtained above by considering the unresummed one-loop correction to the physical quark–quark scattering amplitude. The true high order behavior, however, corresponds to the sum of *all* the possible amplitudes for the process of interest. For this, the actual topographical structure of the diagrams contributing to the amplitude must be properly taken into account. Renormalization scale invariance of the RCC, and the asymptotic freedom property, for an arbitrary choice of covariant gauge, are not confirmed by the diagrammatic calculation of higher order corrections in the case of the quark–quark scattering amplitude considered in this paper.

Gauge dependence of the RCC in QCD has been considered previously in the literature, but usually as an effect only at the two-loop level and at higher orders. It was pointed out that, in the case when the bare parameters of the theory are held fixed, the gauge parameter becomes scale-dependent, and for certain momentum subtraction renormalization schemes, the second coefficient of the beta function

is both scheme- and gauge-dependent [30]. For an arbitrary covariant gauge specified by the fixed parameter ξ , as in the one-loop discussion above, the second beta function coefficient is, however, both gauge and renormalization scheme invariant. Assuming that the RCC, mass and gauge parameter each satisfy renormalization group equations similar to (1.8), and solving the coupled system of differential equations, solutions were found for the RCC that strongly depended on the initial conditions imposed on the running gauge parameter [30]. These solutions exhibit either asymptotic freedom-like behavior or increase with increasing scale until an ultraviolet fixed point is reached [31,32]. As commonly done in the literature, the RCC was treated as an independent mathematical object, without reference to any actual physical process, and the renormalization group equations were assumed to hold without specific diagrammatic justification. It is shown above that, if the RCC is identified with the effective charge of the quark–quark scattering amplitude, the one-loop renormalization group equation* holds only for the specific gauge choice $\xi = -3$. The gauge parameter can then neither vary nor satisfy a RGE.

When quark mass effects are taken into account, the one-loop beta function coefficient is also gauge-dependent, and has a value which depends on the particular n -point Green's function considered for its derivation. The mass-dependent corrections to the triple gluon vertex [33] and the gluon–ghost–ghost vertex [34] are different. A detailed discussion may be found in [35]. A corollary is that the RCC in physical amplitudes is both gauge- and process-dependent at physical scales where quark mass effects (other than those contained in the asymptotically dominant logarithmic terms) are important.

The effective charge (2.7) has been calculated here for the simple case of quark–quark scattering with a unique physical scale $Q = \sqrt{-t}$. In this case the direct physical interpretation as the strength of the interaction between two currents varying as a function of their separation ($\simeq 1/Q$) is particularly transparent. However, since every dressed propagator has just two ends, similar expressions for the RCC (in general, a function of some running loop 4-momentum k) are expected in all physical amplitudes containing virtual gluon lines. Two examples are shown in Fig. 4. Figure 4, *a* shows the three topographically distinct classes of diagrams that contribute to the anomalous magnetic moment of a heavy quark at $O(\alpha_s^3)$. In Fig. 4, *b* the same classes of diagrams are shown for the four-loop photon proper self-energy function due to radiatively corrected quark vacuum polarization loops. As for the quark–quark scattering case, the same topographical structures (giving at most a quadratic dependence on the vertex corrections) are found at all higher orders in the «dressed gluon propagator». The diagrams

*In [31,32] the one-loop RGE was assumed to be gauge-independent and given by the conventional formula (1.10).

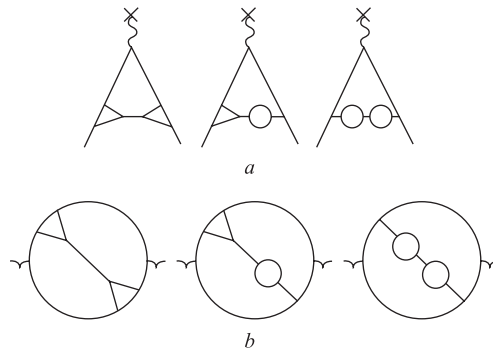


Fig. 4. The topographical structure of diagrams contributing to: *a*) the $O(\alpha_s^3)$ contribution to the anomalous magnetic moment of a quark; *b*) the four-loop photon proper self-energy function

of Fig. 4, *b* are related via the optical theorem and analytical continuation to the process:

$$e^+e^- \rightarrow \gamma^* \rightarrow q\bar{q} + X,$$

where X denotes g , gg or $q'\bar{q}'$.

There has been considerable recent interest in the structure, in high orders of perturbation theory, of diagrams containing chains of vacuum polarization loops in internal gluon propagators (for example, the generalization to higher orders of the $O(\alpha_s^3)$ diagrams with two vacuum polarization loops shown in Fig. 4). The ansatz used for these so-called «renormalon chains» [36] is to replace $n_f/3$ in a calculation considering only n_f different flavors of fermion vacuum polarization loops with $n_f/3 - 11/2 = -\beta_0$. This is clearly a good approximation in the limit $n_f \rightarrow \infty$. As inspection of Fig. 4 shows, however, this will result, in any gauge in which the vertex correction is nonvanishing, in a miscounting of the contribution of the latter, which are included at order n in terms of the form β_0^n , but actually should never appear at higher order than quadratic in the perturbation series. With the gauge choice $\xi = -3$ (loop gauge), however, all vertex corrections vanish and the renormalon chains are correctly given by the above replacement. This gauge choice is, in any case, the one universally (although tacitly) made in all phenomenological applications of the QCD running coupling constant, where renormalization group invariance is assumed. Thus, the «Naive Non-Abelianization» (NNA) ansatz [37] or «Large β_0 Limit» that is typically assumed in phenomenological studies of renormalon effects is a correct one only in loop gauge. The remark that the choice of gauge $\xi = -3$ implies the vanishing of all vertex corrections, has been previously made in the context of two-loop corrections to heavy quark production in e^+e^- annihilation [41].

An instructive example of the inconsistent treatment of Feynman diagrams by the NNA ansatz as well as an illustration of the gauge dependence of fixed order perturbative QCD calculations beyond the next-to-leading order (NLO) is provided by the analysis of the moments of nonsinglet anomalous dimensions of deep-inelastic nucleon structure functions in [38]. In this work the effect of insertion of an arbitrary number of quark or gluon vacuum polarization insertions in the virtual gluon propagator of a forward Compton scattering amplitude (or the equivalent diagrams in the Operator Product Expansion, as in Fig. 1 of [38]) is considered. An example of an $O(\alpha_s)$ diagram that contributes to this amplitude is shown in Fig. 5, *a*. One and two vacuum polarization loop insertions as considered in [38] are shown in the fourth topographical diagrams of Fig. 5, *b* and *d*, respectively. The predictions of this procedure for the loop ($\xi = -3$) and Landau ($\xi = 0$) gauges were compared to the exact massless next-to-next-to-leading-order (NNLO) calculation in Feynman gauge* ($\xi = 1$) of [42]. Table 4, extracted from Table 1 of [38], shows the results of this comparison for the $n = 2$ moment at NLO, as in Fig. 5, *b*, and NNLO, as in Fig. 5, *c* and *d*. In the calculations of [42] the contributions of all 353 Feynman diagrams contributing to the anomalous dimensions up to NNLO were evaluated, whereas in [38] only quark and gluon loop vacuum polarization insertions in Fig. 5, *a* and the other Compton scattering diagrams with one virtual gluon line (see, for example, Fig. 1 of [43]) were considered. Even so, agreement is found with the Loop gauge renormalon calculation at the 20% level at NLO for the $n = 2$ moment. Even better agreement is found for higher moments — it is good at 4.7% for the $n = 6$ moment. However, at NNLO no agreement is found; indeed predictions of the «renormalon dominated» approximation with either choice of gauge have even a different sign to the exact NNLO calculation. The reasonable agreement at NLO between the two calculations when loop gauge is employed in [38] can be understood by inspection of Fig. 5, *b*. This choice of gauge is equivalent, at NLO, to performing a calculation in an arbitrary covariant gauge, in which the non-Abelian one-loop corrections to the quark–gluon coupling are included as well as vacuum polarization insertions. All the NLO vertex and vacuum polarization corrections are included in the topographical diagrams of Fig. 5, *b*. The sum of these contributions is gauge invariant. The situation is quite different at NNLO. The subset of NNLO diagrams shown in Fig. 5, *c*, obtained from those of Fig. 5, *b*

*The formulas given in [42] are actually in Landau gauge. However, it is stated in the paper that for low order moments $n = 2, 4$ «... the diagrams were run with a gauge parameter ξ in the gluon propagator $g_{\mu\nu} - \xi q_\mu q_\nu / q^2$ ». The assumed value (or values) of their parameter ξ ($1 - \xi$ in the notation of the present paper) was not stated and for the moments $n = 6, 8$ the gauge parameter was not included (presumably it was set to zero in the calculations) which corresponds to choosing Feynman gauge. It is assumed here that results compatible with this choice of gauge were also obtained for the $n = 2, 4$ moments.

by inserting an additional virtual gluon between the incoming and outgoing quark lines also gives a gauge invariant result and is correctly described in loop gauge. This is not the case for the diagrams of Fig. 5, *d* — the corresponding sum of the diagrams is of the form $V^2 + 2VL + L^2$, which is manifestly gauge-dependent. Other NNLO contributions with the same color factors as in Table 4 arise from irreducible two-loop vertex and vacuum polarization diagrams. The topographical pattern is the same as in Fig. 5, *b* with the one-loop insertions replaced by irreducible two-loop insertions. As discussed in more detail below, if these two-loop insertions satisfy a Ward identity similar to that respected by the one-loop insertions, this contribution will also be gauge invariant. No possibility exists, however, to remove the gauge dependence of the contribution of the diagrams shown in Fig. 5, *d*. This explains the breakdown of gauge invariance shown by the $C_F C_A^2$ NNLO entries of Table 4.

In an attempt to give a diagrammatic justification of the NNA ansatz, Beneke in [36] considered NLO loop corrections as in Fig. 2, *a* or in Fig. 5, *b* above, for the case of quark pair production by a vector current. Performing the calculation

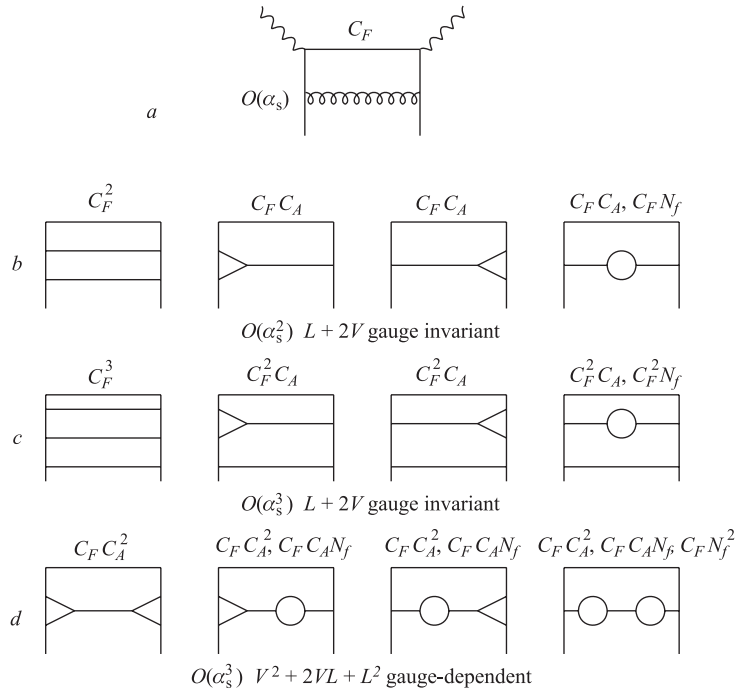


Fig. 5. The topographical structure of diagrams contributing to nonsinglet anomalous dimensions in deep inelastic scattering: *a*) leading order; *b*) next-to-leading order; *c*, *d*) next-to-next-to-leading order. See text for discussion

Table 4. Contributions to the $n = 2$ moment of the nonsinglet anomalous dimension in deep inelastic scattering on a nucleon due to different classes of Feynman diagrams and for different choices of covariant gauge, ξ . See text for discussion

| Gauge | $\gamma_{(1)}(2)$ (NLO) | | $\gamma_{(2)}(2)$ (NNLO) | | |
|-----------------|-------------------------|------------------|--------------------------|---------------|--------------------|
| | $C_F C_A$ | $C_F N_f$ | $C_F C_A^2$ | $C_F C_A N_f$ | $C_F N_f^2$ |
| $\xi = 1$ [42] | 13.9 | $-\frac{64}{27}$ | 117.70 | -38.50 | $-\frac{224}{243}$ |
| $\xi = -3$ [38] | 11.3 | — | -76.0 | 23.0 | — |
| $\xi = 0$ [38] | 7.6 | — | -13.2 | 12.4 | — |

in Landau gauge it was found that the beta function of the corresponding QED calculation was replaced by the one-loop QCD beta function. If this calculation had been performed in an arbitrary covariant gauge, the gauge invariance of the QCD beta function would have been demonstrated. This in no way justifies the general use of the NNA ansatz since manifest gauge dependence as in Fig. 2, *b* or in Fig. 5, *d* first occurs at NNLO where the gauge dependence of the V^2 term is not canceled by NNLO vacuum polarization contributions.

In connection with the work presented in the present paper it is important to notice that the renormalon singularities arise due to loop integrals over the virtuality of an internal photon or gluon line in a Feynman diagram, as in Figs. 4 and 5. Although the renormalon singularities are related to singular IR or UV behavior of the running coupling constant — as discussed by Lautrup in [36], in QED it is the UV Landau singularity — the renormalon singularity occurs for arbitrary values of the external physical scale due to the infinite range of the internal loop momentum*. In contrast, in the simple case of quark–quark scattering discussed in the present paper, there is no integration over the virtuality of the gluon line in which the vertex and loop corrections are inserted and the scale in the running coupling constant is identical to the physical scale of the problem. The diagrammatic analysis shown in Fig. 2 is therefore much simpler and the breakdown of gauge invariance appears as soon as the NNLO contributions of Fig. 2, *b* are evaluated.

*In a discussion of renormalons in a review talk by S.Forte [44] the following important statement can be found: «If the series had alternating signs the singularity (ultraviolet renormalon) would not be on the path of the integral» (in the Borel transform) «but the integral would still run outside the radius of convergence of the series; we will not discuss this any further». This is the only place in the literature, to the present writer’s knowledge, where the limited domain of convergence, in the UV limit, of the QCD RCC (discussed in detail in the present paper) is mentioned. The perturbation series corresponding to the RCC of QCD indeed has «alternating signs».

The classification of diagrams as in Figs. 2, 4 and 5, according to the categories (in an obvious notation) L^n , VL^n , V^2L^n , will remain when L , V are calculated with an arbitrary number of internal lines. The global structure of Eq. (2.5) will then remain the same for calculations including an arbitrary number of loops, though additional nonleading terms in $\ln Q$ will result from integration over internal loops in the basic one-loop vacuum polarization and vertex diagrams shown in Fig. 1.

As in [1], only the leading logarithmic terms in the one-loop correction (and hence in the resummed effective charge) have been taken into account in the above discussion. Constant terms in V and L have been neglected. For a general renormalization scheme, however, constant gauge and renormalization scheme-dependent terms also occur, so that Eq. (3.1) is replaced by the expression:

$$a_Q = a_\mu \frac{\{1 - a_\mu[v(\xi)\lambda + c_v(\xi)]\}^2}{1 + a_\mu[l(\xi)\lambda + c_l(\xi)]}. \quad (4.1)$$

In the \overline{MS} scheme [23]:

$$c_l(\xi) = \frac{10n_f}{9} - \frac{97}{12} - \frac{3}{8}\xi - \frac{3}{16}\xi^2.$$

By a suitable scale choice $\mu = \mu'$ and with $\xi = -3$ Eq. (4.1) may be written as

$$a_Q = \frac{a_{\mu'}}{1 + a_{\mu'} \left[l(-3) \ln \frac{Q}{\mu'} + c_l(-3) \right]}. \quad (4.2)$$

So in this (non-asymptotic) case even in loop gauge the effective charge does not correspond exactly to the solution (1.10) of the one-loop RGE (1.8). Numerically $l(-3) = 3.833$, $c_l(-3) = -3.090$ for $n_f = 5$. Thus, in the \overline{MS} scheme in loop gauge, the resummed one-loop invariant charge is only asymptotically renormalization group invariant when constant terms in the one-loop correction are retained.

Following the observation that the UV divergent parts of the vertex corrections in Fig. 1, b, c may be associated with related diagrams in which the virtual quark propagators are shrunk to a point (or «pinched»), it was suggested [45,46] to redefine a gluon proper self-energy function by adding to the contributions of Fig. 1, $d-g$, that of the pinched vertex diagrams. At one-loop order the resulting gluon proper self-energy function is then gauge invariant. It was then (incorrectly) stated that a gauge invariant resummed gluon propagator may be trivially derived from the one-loop result (for example, Eq. (2.19) of [46]). In fact, it is easy to show, quite generally, that if the one-loop corrected quark-quark scattering amplitude is gauge invariant (the correct initial assumption of the pinch

technique calculations of [45,46]), then resummed amplitudes at all higher orders must be gauge-dependent. Introducing the gauge invariant one-loop quantity:

$$B \equiv L + 2V. \tag{4.3}$$

The resummed amplitude at $O(\alpha_s^{n+2})$ may then be written for $n \geq 1$ (see Fig. 2 and Eq. (2.3)) as

$$\mathcal{M}^{(n+2)} = \mathcal{M}^{(0)}(L + V)^2 L^{n-1}. \tag{4.4}$$

Expressing $\mathcal{M}^{(n+2)}$ in terms of the gauge invariant quantity B and the gauge-dependent quantity $L(\xi)$ gives

$$\mathcal{M}^{(n+2)} = \mathcal{M}^{(0)} \frac{1}{4} (B + L(\xi))^2 L(\xi)^{n-1}, \tag{4.5}$$

which is manifestly gauge-dependent. The Dyson sum in Eq.(2.19) of [34] correctly describes the all orders resummed amplitude, not for an arbitrary gauge parameter ξ , but only for the special choice $\xi = -3$ when $V(\xi) = 0, B = L(-3)$ and

$$\mathcal{M}^{(n+2)} = \mathcal{M}^{(0)} B^{n+1} \quad (\xi = -3). \tag{4.6}$$

Clearly, the above argument for manifest gauge dependence, shown to be valid at the resummed one-loop level must also hold at arbitrary loop order if the vertex and self-energy insertions satisfy a generalized Ward identity giving, at each order of perturbation theory, a condition such as (4.3). It has been shown [47], by the application of background field techniques, that Ward identities relating vertex and self-energy contributions may indeed be derived that are valid to all orders in perturbation theory. The gauge independence of the Ward identity at each fixed order then necessarily implies gauge dependence when the corresponding vertex and self-energy diagrams are resummed.

The manifest gauge dependence of the quark–quark scattering amplitude found, by direct calculation, in this paper, is, apparently, in contradiction with formal proofs [48,49] of the gauge invariance of S -matrix elements in non-Abelian gauge theories. It seems, however, that what is actually proved in these papers is the gauge invariance, at all orders in perturbation theory, of generalized Ward identities. The consequences of *resumming* diagrams of fixed loop order, which as shown above, necessarily generates gauge dependence, were not considered. For example, in the standard reference [49], the Lagrangian from which all the Feynman rules of the theory are derived is introduced, and the change in this Lagrangian due to a change in the gauge parameter is written down. It is then stated that the theory is gauge invariant if such a variation of the gauge parameter leaves S -matrix elements invariant. There immediately follows the statement: «We can formulate this condition» (i.e, that the S -matrix elements are invariant) «in terms of a Ward identity that we have written in terms of the diagrams in Fig. 2». The

unproved and unjustified assertion is thus made that the gauge invariance of a Ward identity is equivalent to gauge invariance of S -matrix elements. This will only be true of unresummed amplitudes at each loop order, not of the resummed amplitudes that, according to quantum mechanical superposition, must exist and are, indeed, essential to generate the RCC. In fact, [49] establishes *only* the gauge invariance of Ward identities, and nothing else. As shown above, it is just the gauge invariance of the unresummed amplitudes that ensures the manifest gauge dependence of the resummed ones. Indeed an S -matrix element (even a formal, generic one) appears nowhere among the equations of [49]. In [48] such a formal S -matrix element does appear, but its gauge invariance properties are derived directly from a Ward identity. No actual physical process, and no effect of resummation, is considered.

By consideration of a subset of n -loop diagrams for the off-shell gluon–gluon scattering amplitude in a noncovariant gauge, it has been claimed [23] to demonstrate that the RCC of QCD is both gauge invariant and process-independent, and that it may be identified with the solution (1.10) of the RGE (1.8). The n -loop diagrams considered are those that may be constructed as a formal «product» of $n + 1$ tree level four-point functions. The diagrams contain both resummed one-loop gluon vacuum polarization and vertex diagrams and a subset of irreducible n -loop diagrams. This set of diagrams cannot, as claimed, be identified with the one-loop RCC in Eq. (1.10), which results solely from the resummation of one-loop (one-particle irreducible) diagrams. At any order in the perturbation series these resummed one-loop diagrams contribute the leading powers of both $\ln Q$ and n_f . They give, in fact, the «renormalon» contribution [36] (see above) that dominates the high order behavior of the perturbation series. The irreducible n -loop ($n > 1$) diagrams of the subset considered in [23] will contribute constant terms or nonleading powers of $\ln Q$, and therefore cannot be identified with terms in the diagrammatic expansion of the RCC in (1.10). Similarly, it has been conjectured (without explicit calculation) in [50] that the «missing» vertex contributions needed to make, say, $\mathcal{M}^{(2)}$ in Eq. (4.5) above, gauge invariant may be derived from «pinch parts» of two-loop irreducible diagrams. This is not possible since the required «missing» contributions contain the factor $(\alpha_s \ln Q)^2$ (see Eq. (2.5)), whereas, as is well known, in both QED [51] and QCD [52] irreducible two-loop vacuum polarization and vertex diagrams have, at most, the next-to-leading logarithmic behavior $\approx \alpha_s^2 \ln Q$. This is easily demonstrated by considering the two-loop solution of the renormalization group equation for the effective charge. In QED, or in QCD in the $\xi = -3$ gauge, Eq. (3.2) generalizes to

$$a_Q = \frac{a_\mu}{1 + a_\mu \beta_0 \lambda + \frac{\beta_1 a_\mu}{\beta_0} \ln(1 + a_\mu \beta_0 \lambda)}, \quad (4.7)$$

where β_1 is the second β -function coefficient. Expanding the right side of Eq. (4.7) up to $O(a_\mu^3)$ yields

$$a_Q = a_\mu \left[1 - a_\mu \beta_0 \lambda + a_\mu^2 \beta_0^2 \lambda^2 - a_\mu^2 \beta_1 \lambda - a_\mu^3 \beta_0^3 \lambda^3 + \frac{3}{2} a_\mu^3 \beta_0^3 \beta_1 \lambda^2 + O(a_\mu^4) \right]. \quad (4.8)$$

It can be seen that β_1 , given by two-particle irreducible vacuum polarization or vertex diagrams, occurs only in sub-leading logarithmic terms of the form $\beta_1 a_\mu^n \lambda^{n-1}$. No possible re-arrangement of these terms can compensate the manifest gauge dependence of the leading-logarithmic terms of the form $(\beta_0 a_\mu \lambda)^n$.

The property exhibited above, for QCD, of gauge dependence of amplitudes on resumming one-loop corrections that, at lowest order, are gauge invariant, is expected to be a general property of non-Abelian gauge theories. In such theories the gauge boson propagator, in an arbitrary covariant gauge is written as [53]

$$P^{\mu\nu}(q^2) = -\frac{i}{q^2 - M^2} \left[g^{\mu\nu} - (1 - \xi) \frac{q^\mu q^\nu}{q^2 - \xi M^2} \right], \quad (4.9)$$

where M is the renormalized gauge boson mass. The topographical structure of diagrams contributing to, say, neutrino–neutrino scattering via Z exchange is the same as that for quark–quark scattering shown in Fig. 1. The one-loop vertex correction containing the non-Abelian ZW^+W^- coupling is gauge-dependent [54]. Since the gauge dependence cancels at lowest order (without resummation) then, just as for QCD, it cannot cancel at any higher order in the resummed one-loop amplitude. Indeed a similar conclusion as to the necessity of the $\xi = -3$ gauge in order to obtain an effective charge that satisfies a RGE, reached in this paper for QCD, has previously been obtained, for the case of the Weinberg–Salam model, by Baulieu and Coquereaux [55]. These authors pointed out that, with the special gauge choice (in the notation of the present paper) $\xi = -3$, the renormalization constant of the $Z - \gamma$ mixing term vanishes, so that, in this case, effective charges satisfying separate (decoupled) RGEs may be associated with the one-loop resummed photon and Z -boson propagators. It is also interesting to note that $\xi = -3$ is the unique choice of covariant gauge for which the photon mass counterterms in the renormalized Lagrangian vanish. The case of W exchange was not considered, but (as may be seen by inspection of the relevant formula given, in an arbitrary covariant gauge, in [56]) the choice $\xi = -3$ results in the vanishing of the renormalization constants associated with the one-loop vertex corrections to both Z and W exchange fermion–fermion scattering amplitudes. As for the QCD case considered in the present paper, it is then expected that, only for this special choice of gauge, an effective charge satisfying a RGE may be associated with the resummed W propagator.

The pinch technique, and similar methods to formally shift gauge-dependent pieces between diagrams, have also been applied to electroweak amplitudes [40,

46–49]. Although gauge invariant boson proper self-energy functions may be defined at one-loop level, any resummed higher order amplitude is demonstrably gauge-dependent, by the same argument as that given above for QCD. So, although for a particular choice of gauge parameter (such that the sum of all vertex corrections vanishes) resummed W and Z running propagators may be defined that satisfy a RGE, they cannot, contrary to the claim of [40, 46–49], be so defined in a gauge invariant manner. The diagrammatic inconsistency of these procedures is made manifest by the inclusion in the modified vector boson self-energy function of box diagram contributions. If the effective charge is expanded as a perturbation series, the box diagram contributions at each order will give terms of a geometric series. There is no way that such a series can be meaningfully interpreted in terms of a sum of such diagrams required by quantum mechanical superposition. In fact, the contributions to physical amplitudes of box diagrams can be systematically resummed [60–62], but the result found is typically the exponential of a double logarithm of the relevant physical scale, not the sum of a geometric series. For the case of the fermion–fermion scattering amplitude the contribution of box diagrams is expected to be important only in the $|t| \rightarrow 0$ limit and to vanish [56] in the $|t| \rightarrow \infty$ limit.

A discussion of the gauge dependence, beyond one-loop order, of the resonant Z -boson amplitude, may be found in [63].

The limited convergence domain imposed by requiring finiteness of the geometric series, which occurs in all theories in which the RCC decreases with increasing scales, can be avoided by choosing a very high renormalization scale*. This is equivalent, for such theories, to the choice, in QED, of on-shell renormalization, yielding a RCC that is convergent for all scales below the Landau scale [20]. Although such a choice guarantees convergence for all physical scales below the chosen renormalization point, it appears artificial from a physical viewpoint. If a strong interaction process at, say, the scale of the mass of the charm quark is to be described using a renormalization point at the GUT scale Q_{GUT} , the formula for the RCC at scale m_c will depend upon the masses of all strongly interacting elementary particles below Q_{GUT} and above m_c . There will be a phenomenon of «inverse decoupling» whereby the lower the scale the more high mass particles must be taken into account. Feynman amplitudes using such a renormalization scale would lose their correspondence (valid in the on-shell scheme) with space–time processes. With on-shell renormalization, the decoupling of heavy particles at low scales is understood in terms of a natural hierarchy of physical scales. It seems reasonable that the physics of the strong interaction at the scale of the charm quark mass, m_c , should be independent of the value of the top quark mass, m_t , when $m_t \gg m_c$. According to the Uncertainty Principle, the

*I am indebted to W. Beenakker for this remark.

contribution to vacuum polarization loops of particles with masses much greater than the propagator virtuality is expected to correspond to short lifetime fluctuations giving only a small contribution to the radiative correction. This is no longer the case if the RCC is renormalized at scales $\gg m_t$.

An enormously successful phenomenology of the strong interaction has been developed over the past three decades based on perturbative QCD. Many aspects of QCD, such as the existence of the color quantum number of spin-one gluons with self-coupling, the predicted values of color factors, and a coupling constant that decreases with increasing scales in the experimentally accessible region, are confirmed, beyond doubt, experimentally [64]. However, it might be hoped that the physical predictions of a candidate gauge *theory* would be gauge invariant at all orders in perturbation theory, as is the case in QED. Explicit calculation for the current non-Abelian gauge theories (both QCD and electroweak theory), as reviewed in the present paper, seems to show, however, that this is not the case. The point with error bars at $Q = 90$ GeV on the loop gauge curve in Fig. 3 shows the uncertainty on α_s (± 0.005) of an early measurement using hadronic Z decays at LEP [65]. The input value $\alpha_s(5 \text{ GeV}) = 0.2$ has been chosen to be consistent with deep inelastic scattering measurements [66]. If the asymptotic running coupling constant with time-like argument measured at LEP at the scale $Q = M_Z$ has a similar value to $\alpha_s^{\text{eff}}(Q)$ for space-like argument considered in this paper, it is clear from Fig. 3 that the *measured* value of the gauge parameter must be close to -3 .

On a more positive note, the phenomenological success, in QCD, of calculations based on the renormalization group, as well as of «renormalon» based models, both of which are shown here to require the use of the $\xi = -3$ gauge, suggests that further understanding requires a deeper theoretical explanation of nature's apparent choice of this gauge (see Fig. 3). The question is, why, in non-Abelian theories, do UV divergent loop diagrams apparently acquire logarithmic corrections after renormalization but not similar vertex diagrams? Since the non-Abelian triple gluon vertex occurs in both loop (vacuum polarization) and vertex insertions it seems that consistency with experiment requires the cancellation of vertex contributions when summed over the complete particle content of the theory. That is, in some conjectured modified version of QCD, complete cancellation of triangle vertex insertions similar to the anomaly cancellation provided by the particle content of the fermion families of the Standard Model. However, consistency with the diagrammatic description (i.e., with quantum mechanical superposition) must always limit the scale-range of applicability of the RCC due to the convergence properties of geometric series.

Finally, two important caveats concerning the work presented in this paper should be mentioned. Firstly, only covariant gauges specified by the parameter ξ are considered, whereas certain noncovariant gauges [67] such as axial gauge ($A_3 = 0$) or light-cone gauge ($n_\mu A^\mu = 0$, $n^2 = 0$) are frequently employed in

QCD phenomenology. The second concerns the recently developed successful application of Analytical Perturbation Theory (APT) to QCD phenomenology [68]. In order to avoid infra-red divergences when $\Lambda \rightarrow 0$ in the conventional QCD perturbation series for the RCC, APT introduces, by way of the Källén–Lehmann spectral representation of the dressed gluon propagator, the condition of analyticity in the Q^2 variable. This also imposes a causality requirement. In this case, the correspondence between the so-obtained «Euclidean running couplant», α_E , and the sum of a QCD perturbation series, in which the terms represent the contribution of specific Feynman diagrams, breaks down. No statements may then be made concerning the gauge dependence and convergence properties of α_E .

Acknowledgements. I wish to thank, especially, W. Beenakker for his careful reading of an early version of this paper and for constructively critical comments. Discussions with M. Consoli are also gratefully acknowledged. I thank M. Veltman for pointing out to me the work contained in [49], and an anonymous referee for introducing me to the related work of Mikhailov discussed in Sec. 4.

APPENDIX

The sum of the first n terms of a geometric series with a negative common ratio $r = -|r|$ is given by the relation [24]:

$$S_n = 1 - |r| + |r|^2 - \dots + (-|r|)^{n-1} = \frac{1 - (-|r|)^n}{1 + |r|}. \quad (\text{A.1})$$

It follows that

$$S_n = \frac{1 + |r|^n}{1 + |r|} \quad (n - \text{odd}), \quad (\text{A.2})$$

$$S_n = \frac{1 - |r|^n}{1 + |r|} \quad (n - \text{even}). \quad (\text{A.3})$$

If $|r| < 1$, then $S_\infty \equiv (\text{limit as } n \rightarrow \infty \text{ of } S_n) = 1/(1 + |r|)$. If $|r| = 1$, then $S_n = 1$ for n odd and $S_n = 0$ for n even. If $|r| > 1$, $S_\infty = +\infty$ for n odd and $S_\infty = -\infty$ for n even.

Table 5 presents values of S_n versus n , demonstrating the convergence of the series for $|r| = 1/2$ and its divergence for $|r| = 2$. The Dyson sum of

Table 5. Values of the sum, S_n , of first n terms of the geometric series in (A.1) for $|r| = 1/2$ (convergent series) and $|r| = 2$ (divergent series)

| n | 2 | 3 | 4 | 5 | 6 | 7 | 9 | $1/(1 + r)$ |
|-------------|-----|------|-------|-------|-------|-------|-------|---------------|
| $ r = 1/2$ | 0.5 | 0.75 | 0.625 | 0.688 | 0.656 | 0.673 | 0.664 | 0.667 |
| $ r = 2$ | -1 | 3 | -5 | 11 | -21 | 43 | -85 | 0.333 |

vacuum polarization insertions in the gluon propagator in QCD gives a geometric series similar to (A.1) above. The impossibility of «asymptotic freedom», which conjectures that $S_n \rightarrow 0$ as $n \rightarrow \infty$ is evident from inspection of (A.2) and (A.3) above and Table 5.

REFERENCES

1. *Coqueroaux R., De Rafael E.* // Phys. Lett. B. 1977. V. 69. P. 181.
2. *Ellis R. K. et al.* // Nucl. Phys. B. 1980. V. 173. P. 397.
3. *Slominski W., Furmanski W.* Krakow Preprint TPJU-11/81. 1981.
4. *Ellis R. K., Sexton J. C.* // Nucl. Phys. B. 1986. V. 269. P. 445.
5. *Korthals Altes C. P., De Rafael E.* // Phys. Lett. B. 1976. V. 62. P. 320; Nucl. Phys. B. 1977. V. 125. P. 275.
6. *'tHooft G., Veltman M.* // Nucl. Phys. B. 1972. V. 44. P. 189.
7. *Stückelberg E. C. G., Peterman A.* // Helv. Phys. Acta. 1953. V. 26. P. 499.
8. *Gell-Mann M., Low F.* // Phys. Rev. 1954. V. 95. P. 1300.
9. *Bogoliubov N. N., Shirkov D. V.* // Nuovo Cim. 1956. V. 3. P. 845.
10. *Callan C., Jr.* // Phys. Rev. D. 1970. V. 2. P. 1541.
11. *Symanzik K.* // Commun. Math. Phys. 1970. V. 18. P. 227; 1971. V. 23. P. 49.
12. *Field R. D.* Applications of Perturbative QCD. Redwood City, California: Addison-Wesley, 1989. Ch. 6.
13. *Pennington M.* // Rep. Prog. Phys. 1983. V. 46. P. 393.
14. *Itzykson C., Zuber J.-B.* Quantum Field Theory. N. Y.: Mc Graw Hill, 1985.
15. *Field J. H.* // Ann. Phys. (N. Y.). 1993. V. 226. P. 209.
16. *Field J. H.* // Intern. J. Mod. Phys. A. 1994. V. 9. P. 3283.
17. *Lee T. D., Nauenberg M.* // Phys. Rev. 1964. V. 133. P. 1549.
18. *Kinoshita T.* // J. Math. Phys. 1962. V. 3. P. 650.
19. *Field J. H.* // Mod. Phys. Lett. A. 1996. V. 11. P. 2921.
20. *Field J. H.* // Intern. J. Mod. Phys. A. 2000. V. 15. P. 3245.
21. *Field J. H.* <http://xxx.lanl.gov/abs/hep-ph/9811399v1>, 9811399v2
22. *Böhm M., Denner A., Hollik W.* // Nucl. Phys. B. 1988. V. 304. P. 687.
23. *Watson N. J.* // Nucl. Phys. B. 1997. V. 494. P. 388.
24. *Hardy G. H.* Pure Mathematics. Cambridge Univ. Press, 1955. P. 149.
25. *Abrikosov A. A., Khalatnikov I. M., Landau L. D.* // Dokl. Akad. Nauk. SSSR. 1954. V. 95. P. 177. English transl.: Collected Papers of L. D. Landau / Ed. D. ter Haar. Oxford, 1965.

26. *Georgi H., Glashow S.L.* // Phys. Rev. Lett. 1974. V. 32. P. 438.
27. *Georgi H., Quinn H.R., Weinberg S.* // Ibid. V. 33. P. 451.
28. *Gross D., Wilczek F.* // Phys. Rev. Lett. 1973. V. 30. P. 1343.
29. *Politzer H.D.* // Ibid. P. 1346.
30. *Espriu D., Tarrach R.* // Phys. Rev. D. 1982. V. 25. P. 1073.
31. *Rączka P.A., Rączka R.* // Phys. Rev. D. 1989. V. 39. P. 643.
32. *Tarasov O.V., Shirkov D.V.* // Sov. J. Nucl. Phys. 1990. V. 51. P. 877.
33. *Nachtmann O., Wetzel W.* // Nucl. Phys. B. 1979. V. 146. P. 273.
34. *Georgi H., Politzer H.D.* // Phys. Rev. D. 1976. V. 14. P. 1829;
Politzer H.D. // Nucl. Phys. B. 1976. V. 146. P. 283.
35. *Coqueroaux R.* // Phys. Rev. D. 1981. V. 23. P. 1365.
36. *Lautrup B.* // Phys. Lett. B. 1977. V. 69. P. 107.
'tHooft G. The Whys of Subnuclear Physics // Proc. of the 15th Intern. School of Subnuclear Physics, Erice, Sicily, 1977 / Ed. A. Zichichi. N. Y., 1979. For references to more recent work see, for example, *Beneke M.* // Phys. Rep. 1999. V. 317. P. 1.
37. *Broadhurst D.J., Grazin A.G.* // Phys. Rev. D. 1995. V. 52. P. 4082.
38. *Mikhailov S.V.* // Phys. Lett. B. 1998. V. 431. P. 387.
39. *Beneke M., Braun V.M.* Renormalons and Power Corrections // Physics Handbook of QCD / Ed. M. Shifman. Singapore: World Sci., 2001.
40. *Braun V.M., Gardi E., Gottwald S.* // Nucl. Phys. B. 2004. V. 685. P. 171.
41. *Chetyrkin K.G. et al.* // Phys. Lett. B. 1996. V. 384. P. 233.
42. *Larin S.A., van Ritbergen T., Vermaseren J.A.M.* // Nucl. Phys. B. 1994. V. 427. P. 41.
43. *Mankiewicz L., Maul M., Stein E.* // Phys. Lett. B. 1997. V. 404. P. 387.
44. *Forte S.* Progress in Perturbative QCD // Proc. of the 5th Intern. Workshop on Deep-Inelastic Scattering and QCD-DISC'97, Chicago, IL, USA, April 14-18, 1997. N. Y., 1997; hep-ph/9706390.
45. *Cornwall J.M.* // Phys. Rev. D. 1982. V. 26. P. 1453.
46. *Cornwall J.M., Papavassiliou J.* // Phys. Rev. D. 1989. V. 40. P. 3474.
47. *Denner A., Weiglein G., Dittmaier S.* // Phys. Lett. B. 1996. V. 333. P. 420.
48. *Lee B.W., Zinn-Justin J.* // Phys. Rev. D. 1973. V. 7. P. 1049;
Abers E., Lee B.W. // Phys. Rep. C. 1973. V. 9. P. 127.
49. *'tHooft G., Veltman M.* // Nucl. Phys. B. 1972. V. 50. P. 318.
50. *Papavassiliou J., Pilaftsis A.* // Phys. Rev. D. 1996. V. 53. P. 2128.
51. *Jost R., Luttinger J.M.* // Helv. Phys. Acta. 1950. V. 23. P. 201.
52. *Jones D.R.T.* // Nucl. Phys. B. 1974. V. 75. P. 531.

53. 'tHooft G. // Nucl. Phys. B. 1971. V. 35. P. 167.
54. Degrassi G., Sirlin A. // Nucl. Phys. B. 1992. V. 383. P. 73.
55. Baulieu L., Coquereaux R. // Ann. Phys. 1982. V. 140. P. 163.
56. Kuroda M., Moulataka G., Schildknecht D. // Nucl. Phys. B. 1991. V. 350. P. 251.
57. Kennedy D. C. et al. // Nucl. Phys. 1989. V. 321. P. 83;
Kennedy D. C., Lynn B. W. // Ibid. V. 322. P. 1.
58. Degrassi G., Sirlin A. // Phys. Rev. D. 1992. V. 46. P. 3104.
59. Papavassiliou J., De Rafael E., Watson N. J. // Nucl. Phys. B. 1997. V. 503. P. 79.
60. Lepage G. P., Brodsky S. J. // Phys. Lett. B. 1979. V. 87. P. 359.
61. Chase M. K. // Nucl. Phys. B. 1981. V. 189. P. 461.
62. Photiadis D. M. // Phys. Lett. B. 1985. V. 164. P. 160.
63. Passera M., Sirlin A. // Phys. Rev. Lett. 1996. V. 77. P. 4146.
64. See, for example, the Proc. of the Workshop «QCD 20 Years Later», Aachen, 1992 / Eds. Zerwas P. M., Kastrup H. A. Singapore: World Sci., 1993.
65. The LEP Electroweak Working Group. A Combination of Preliminary LEP Electroweak Measurements and Constraints on the Standard Model. CERN-PPE/95-172.
66. Virchaux M., Milsztajn A. // Phys. Lett. B. 1992. V. 274. P. 221.
67. Jackson J. D., Okun L. B. // Rev. Mod. Phys. 2001. V. 73. P. 663.
68. Shirkov D. V., Solovtsov I. L. // Theor. Math. Phys. 2007. V. 150. P. 132, and references therein.